J. Biochem. 130, 439–447 (2001)

Effects of Five-Tryptophan Mutations on Structure, Stability and Function of *Escherichia coli* Dihydrofolate Reductase[1]

Eiji Ohmae, Yoshie Sasaki, and Kunihiko Gekko[2]

Department of Mathematical and Life Sciences, Graduate School of Science, Hiroshima University, Higashi-Hiroshima 739-8526

Received May 30, 2001; accepted June 29, 2001

To elucidate the roles of tryptophan residues in the structure, stability, and function of *Escherichia coli* dihydrofolate reductase (DHFR), its five tryptophan residues were replaced by site-directed mutagenesis with leucine, phenylalanine or valine (W22F, W22L, W30L, W47L, W74F, W74L, W133F, and W133V). Far-ultraviolet circular dichroism (CD) spectra of these mutants reveal that exciton coupling between Trp47 and Trp74 strongly affects the peptide CD of wild-type DHFR, and that Trp133 also contributes appreciably. No additivity was observed in the contributions of individual tryptophan residues to the fluorescence spectrum of wild-type DHFR, Trp74 having a dominant effect. These single-tryptophan mutations induce large changes in the free energy of urea unfolding, which showed values of 1.79–7.14 kcal/mol, compared with the value for wild-type DHFR of 6.08 kcal/mol. Analysis of CD and fluorescence spectra suggests that thermal unfolding involves an intermediate with the native-like secondary structure, the disrupted Trp47-Trp74 exciton coupling, and the solvent-exposed Trp30 and Trp47 side chains. All the mutants except W22L (13%) retain more than 50% of the enzyme activity of wild-type DHFR. These results demonstrate that the five tryptophan residues of DHFR play important roles in its structure and stability but do not crucially affect its enzymatic function.

Key words: dihydrofolate reductase, enzyme function, point mutations, structural stability, tryptophan residues.

Dihydrofolate reductase (DHFR) [EC 1.5.1.3] from *Escherichia coli* is a monomeric protein of 159 amino acids with no disulfide bond or prosthetic group. Three-dimensional structure of the enzyme in the crystalline state was determined for the apoenzyme (*1*) and many enzyme-ligand complexes (*2–6*). However, the conformation of DHFR in solution has remained largely unresolved, as shown by many spectroscopic data (*7–9*), enzyme kinetics (*10–12*), and equilibrium and kinetic unfolding-refolding analyses (*13–21*). There are at least two conformers with different affinities for cofactor and substrate (*8*, *10*, *22*, *23*). The far-ultraviolet circular dichroism (CD) spectrum of DHFR is surprisingly influenced by mutations, although it retains the native conformation and the enzyme activity (*24–28*). Kuwajima *et al.* constructed a W74L mutant of DHFR and showed that the side chains of Trp47 and Trp74 form an exciton coupling to affect the far-ultraviolet CD spectrum (*15*). As shown in Fig. 1, DHFR has five tryptophan residues, and the side chains of Trp47 and Trp74 make close contact. The other three tryptophans (Trp22, Trp30, and Trp133) are separated from each other by greater distances, but Grishina and Woody theoretically predicted their contribution to the peptide CD (*29*). Recently, we found that the far-ultraviolet CD spectrum of DHFR is also modified by mutations at positions 67 and 121, where the side chains are buried in the interior of the enzyme molecule, but not by mutations at position 145, where the side chain is exposed to the solvent (*24–26*).

The spectrum of DHFR is not only altered by amino acid substitution but is also temperature-dependent. Far-ultraviolet CD and fluorescence spectra show the large temperature dependence of the native state (*30*). Interestingly, these spectroscopic changes correlate clearly with the temperature dependence of the partial specific volume and adiabatic compressibility, which is two or threefold larger than those of other globular proteins (*31*). Thermal unfolding of DHFR involves at least one intermediate, in which certain tryptophan residues are exposed at low temperature (*30*). These results suggest that the conformation of DHFR is highly flexible, and a small alteration of tertiary structure by mutation or temperature change extends to the vicinity of tryptophan residues via the modified atomic packing or long-range interaction. However, it is unknown which tryptophan residues are responsible for such spectroscopic properties and to what extent individual tryptophan residues affect the tertiary structure and function of DHFR, because only limited mutation studies have been performed on the tryptophan residues. (*15*, *32*).

To address this problem, in the present study the five tryptophan residues of DHFR were replaced by site-directed mutagenesis with leucine, phenylalanine or valine

[1] This work was supported by a Grant-in-Aid for Scientific Research from the Ministry of Education, Science, Sports and Culture of Japan (No. 10480159).

[2] To whom correspondence should be addressed.

Abbreviations: CD, circular dichroism; DHFR, dihydrofolate reductase; EDTA, ethylenediaminetetraacetic acid; NADPH, nicotinamide adenine dinucleotide phosphate (reduced form).

© 2001 by The Japanese Biochemical Society.

Downloaded from http://jb.oxfordjournals.org/ at Islamic Azad University on September 30, 2012

(W22F, W22L, W30L, W47L, W74F, W74L, W133F, and W133V). The role of individual tryptophan residues in the structure, stability and function of DHFR will be discussed in terms of the difference CD and fluorescence spectra, free energy of urea unfolding, thermal unfolding, and enzymatic activity.

MATERIALS AND METHODS

Plasmid and Mutant Constructions—All mutant DHFR genes were constructed with plasmid pTZwt1-3 (3.7 kb), which produced 1,400-fold overexpression of the wild-type DHFR protein (*33*). For site-directed mutagenesis, the following seven oligonucleotides were synthesized in a three-step PCR reaction as described previously (*27*): 5′GAGATCGGCCGGCAGGTTWAATGGCATGGCGTTTTC3′ (pW22FL); 5′GTTGCGTTTAAAWAAGGCGAGATCGGCCGGCAGGTT3′ (pW30FL); 5′AGGCCTACCGATCGATTCWAAGGTATGGCGCCCCAT3 (pW47FL); 5′GGCCGCGATCGCTTCGTCGACCGATTTAACWAAGGTAACCCG3′ (pW74FL); 5′CCGGATGACTTWGAATCGGTATTCAGCGAATTTCATGATGCT3′ (pW133FL); 5′GGGGATCCGCTCTTGACAATTAGTTAACTATTTGT3′ (pWT-F); and 5′GAGGATCCTTAACGACGCTCGAGGATTTCGAAACA3′ (pWT-BC), where W is a mixture of adenine (A) and thymine (T). The mutant DHFR genes obtained were digested with *Bam*HI, cloned into pUC118 (*34*), and sequenced with a Perkin Elmer Applied Biosystems Model 373A DNA sequencer. An unexpected mutation to valine instead of leucine occurred at position 133, probably because of misreading in the multiple PCR reaction.

Protein Purification—The wild-type and mutant DHFR proteins were purified as described previously (*26*). The concentration of wild-type DHFR was determined using a molar extinction coefficient of 31,100 $M^{-1}\cdot cm^{-1}$ at 280 nm (*10*). The concentrations of mutant DHFRs were determined assuming the following molar extinction coefficients ($M^{-1}\cdot cm^{-1}$) at 280 nm: 24,690 (W22F), 24,240 (W22L), 25,810 (W30L), 24,040 (W47L), 26,870 (W74F), 26,630 (W74L), 25,420 (W133F), and 27,620 (W133V). These values were estimated from the intrinsic fluorescence intensity of tryptophan residues in 5.8 M urea solution, on the assumption that the mutant DHFRs would be fully unfolded and all the tryptophan side chains exposed to the solvent.

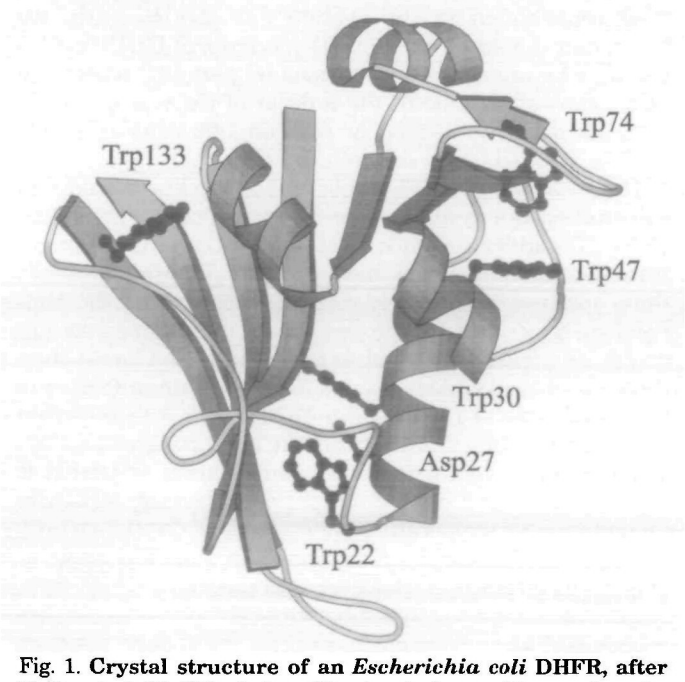

Fig. 1. **Crystal structure of an *Escherichia coli* DHFR, after Bolin *et al.* (2).** Side chains of five tryptophan residues and a catalytic residue, Asp27, are shown by ball-and-stick model. This figure was produced using the graphics program Molscript (*45*). The α-carbons of Trp22, Trp30, Trp47, Trp74, and Trp133 residues are separated by 5, 10, 19, 27, and 22 Å, respectively, from the α-carbon of Asp27.

Circular Dichroism Spectra—Far-ultraviolet CD spectra of the wild-type and mutant DHFRs were measured at 15°C using a Jasco J-720W spectropolarimeter as described previously (*26*). The solvent was 10 mM potassium phosphate (pH 7.0) containing 0.1 mM EDTA and 0.1 mM dithiothreitol. The protein concentration was kept at about 20 μM.

Fluorescence Spectra—Fluorescence emission spectra of the wild-type and mutant DHFRs were measured using a Jasco FP-750 spectrofluorometer in the wavelength region from 300 to 450 nm at 15°C. The excitation wavelength was 290 nm and the slit width was 5 nm. The solvent was the same as for the CD measurements. The protein concentration was 0.5 μM.

Equilibrium Urea Unfolding—Equilibrium unfolding of DHFRs with urea (ultrapure product from Schwarz/Mann) was monitored by the molar elipticity at 222 nm and 15°C with a Jasco J-720W spectropolarimeter as described previously (*26*). The solvent was 10 mM potassium phosphate (pH 7.0) containing 0.1 mM EDTA and 0.1 mM dithiothreitol. The protein concentration was kept at about 20 μM. All samples were fully equilibrated at each denaturant concentration before the CD measurements. The observed molar ellipticity data, [θ] (30–40 points), were directly fitted to the two-state unfolding model, native (N) <——> unfolded (U), by means of nonlinear least-squares regression analysis with the SALS program (*35*), as follows

$$[\theta] = ([\theta]_N + [\theta]_U \exp(-\Delta G_u/RT))/(1 + \exp(-\Delta G_u/RT)) \quad (1)$$

where ΔG_u is the Gibbs free energy change of unfolding, R the gas constant, T the absolute temperature, and $[\theta]_N$ and $[\theta]_U$ the molar ellipticities of the native and unfolded forms, respectively. $[\theta]_N$ and $[\theta]_U$ at a given urea concentration were estimated by assuming the same linear dependence of ellipticity in the transition region as in the pure native (pre-transition region) and unfolded states (post-transition region). The free energy change of unfolding, ΔG_u, in Eq. 1 was assumed to be linearly dependent on the urea concentration (*36*)

$$\Delta G_u = \Delta G^\circ_u + m[\text{urea}] \quad (2)$$

where ΔG°_u is the free energy change of unfolding in the absence of a denaturant, and the slope, m, is a parameter reflecting the cooperativity of the transition. The urea concentration at the mid-point of the transition ($\Delta G_u = 0$) was defined as C_m.

Thermal Unfolding—Thermal unfolding of DHFRs was monitored by CD and fluorescence spectra using a Jasco J-720W spectropolarimeter and a Jasco FP-750 spectrofluorometer, at the protein concentrations of 5 and 0.5 μM,

Downloaded from http://jb.oxfordjournals.org/ at Islamic Azad University on September 30, 2012

respectively. The solvent was the same as those for the CD spectra measurements. Temperature of the sample was controlled with a thermobath circulator (NESLAB RTE-110) and measured within an accuracy of ± 0.1°C using a digital thermometer (Takara Kogyo, D221), which was connected to a sensor set in the top part of the sample solution. The CD and fluorescence spectra at each temperature were recorded as an equilibrium value 15 min after each temperature change.

Specific Activity—Specific activity of the wild-type and mutant DHFRs was measured spectrophotometrically using a Jasco V-520 spectrophotometer at 25°C. The buffer used was 33 mM succinic acid containing 44 mM imidazole and 44 mM diethanolamine, whose pH was adjusted to 7.0 with acetic acid or tetraethylammonium hydroxide. The concentrations of dihydrofolate (Sigma) and NADPH (Oriental Yeast) were determined spectrophotometrically using molar extinction coefficients of 28,000 $M^{-1}\cdot cm^{-1}$ at 282 nm and 6,200 $M^{-1}\cdot cm^{-1}$ at 339 nm, respectively. The enzyme concentration was determined from the absorbance at 280 nm. The final concentrations of dihydrofolate, NADPH, and enzymes were 50 μM, 60 μM, and 60–90 nM, respectively. The initial velocities of the enzyme reaction were calculated from the time course of absorbance at 340 nm using a differential molar extinction coefficient of 11,800 $M^{-1}\cdot cm^{-1}$ (*37*).

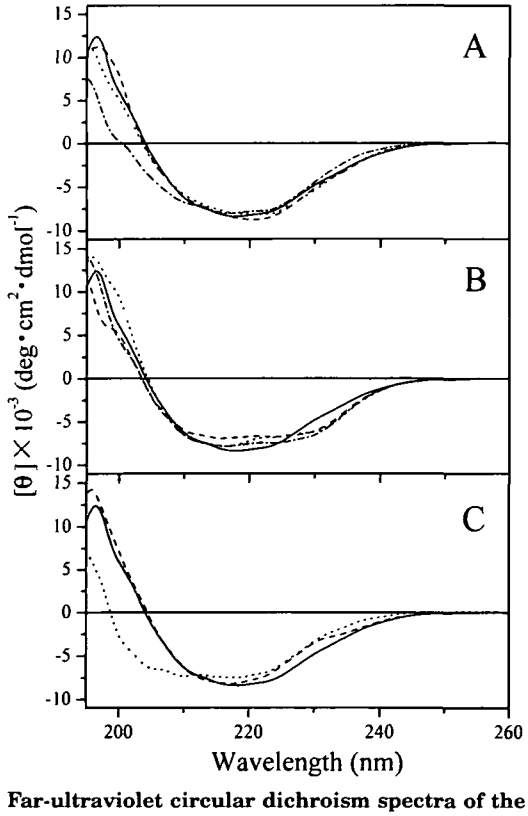

Fig. 2. **Far-ultraviolet circular dichroism spectra of the wild-type and mutant DHFRs at 15°C.** The solvent used was 10 mM potassium phosphate (pH 7.0) containing 0.1 mM EDTA and 0.1 mM dithiothreitol. (A): (——) Wild-type DHFR; (– – – –) W22F; (------) W22L; (–·–·–) W30L. (B): (——) Wild-type DHFR; (– – – –) W47L; (------) W74F; (–·–·–) W74L. (C): (——) Wild-type DHFR; (– – –) W133F; (------) W133V.

RESULTS

Circular Dichroism Spectra—Figure 2 shows far-ultraviolet CD spectra of the wild-type and mutant DHFRs at 15°C and pH 7.0. The CD spectra of all the mutants except W22F and W22L are clearly different from those of wild-type DHFR, suggesting that all tryptophan residues except Trp22 contribute to some extent to the peptide CD of the wild-type DHFR. The large decrease in CD intensity at 200–213 nm for W30L (Fig. 2A) is thought to due not to unfolding but to local structural change of the native form, since the unfolded fraction of this mutant is negligibly small in the absence of urea as shown in Fig. 4. Three mutants, W47L, W74F, and W74L, show characteristic CD spectra compared with wild-type DHFR (Fig. 2B): the ellipticity is higher and lower, respectively in the wavelength regions below and above 225 nm. This result is consistent with the previous observation for W74L mutant (*15*), and clearly indicates that exciton coupling between Trp47 and Trp74 side chains contributes greatly to the far-ultraviolet CD spectrum of wild-type DHFR. In contrast to other mutants, W133F shows a large increase in ellipticity at 212–250 nm accompanying a shoulder at around 235 nm (Fig. 2C). The large decrease in CD intensity of W133V over the whole range of wavelength might be partly ascribed to unfolding of the mutant at this temperature, as revealed by the fluorescence spectra and the urea unfolding experiments.

Fluorescence Spectra—Figure 3 shows fluorescence emission spectra of the wild-type and mutant DHFRs at 15°C and pH 7.0. As expected from the reduction of a tryptophan residue, all the mutants except W133V show decreased fluorescence intensity. Five mutants, W22L, W22F, W30L, W47L, and W133F, show reduced peak intensity of 86–97% of that of wild-type DHFR, and in four cases a small red shift from 343 nm (wild) to 344 nm (W22F and W133F) and 345 nm (W22L and W30L). However, much more significant changes are observed for mutants W74F and W74L:

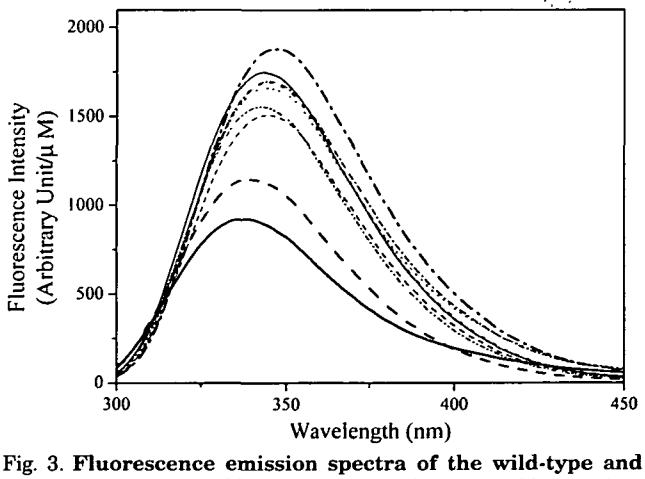

Fig. 3. **Fluorescence emission spectra of the wild-type and mutant DHFRs at 15°C.** The solvent used was 10 mM potassium phosphate (pH 7.0) containing 0.1 mM EDTA and 0.1 mM dithiothreitol. The excitation wavelength was 290 nm. The width of the excitation and emission slits was 5 nm. (——) Wild-type DHFR; (– – – –) W22F; (------) W22L; (–·–·–) W30L; (·····) W47L; (——) W74F; (– – –) W74L; (••••) W133F; (—·—·) W133V.

Downloaded from http://jb.oxfordjournals.org/ at Islamic Azad University on September 30, 2012

the peak intensity is only 53 and 66% of that of wild-type DHFR at the peak wavelength of 338 and 339 nm, respectively. These results suggest that Trp74 of the five tryptophan residues contributes most significantly to the fluorescence spectrum of wild-type DHFR. Mutant W133V show a red-shift to the peak wavelength of 348 nm and a large increase in fluorescence intensity, indicating that this mutant is partially unfolded and some tryptophan side chains are exposed to the solvent under the experimental conditions used.

Equilibrium Urea Unfolding—To clarify the effects of tryptophan residues on the structural stability, equilibrium urea unfolding was studied by monitoring the molar ellipticity at 222 nm. Figure 4 shows typical plots of the apparent unfolded fraction of the wild-type and six mutant DHFRs as a function of urea concentration at 15°C and pH 7.0. Similar transition curves are also observed for other two mutants, W22F and W133F (data not shown). All the transition curves shift to lower urea concentration, suggesting the destabilized structure of these mutants. The W133V mutant has extremely low stability, because it is partly unfolded even in the absence of urea.

Unfolding of all mutants follows a two-state transition model (Fig. 4), as found for the wild-type and mutant DHFRs at other positions (*25–27*). This is also supported by the observation that the CD spectra of these mutants in urea solutions have an isoellipticity point at around 210 nm (data not shown). The Gibbs free energy change of unfolding (ΔG_u) was calculated using Eq. 1 and plotted against the urea concentration in the inset of Fig. 4. The good linear relationship observed allows us to calculate the free energy change of unfolding in the absence of urea, ΔG°_u, the slope, m, and the urea concentration at $\Delta G_u = 0$, C_m (see Eq. 2). The results of the calculations are listed in Table I. Interestingly, the single-tryptophan mutations induce large changes in ΔG°_u (1.79–7.14 kcal/mol) and in m (−1.29 to −2.60 kcal/mol·M) from the corresponding values for wild-type DHFR (6.08 kcal/mol and −1.96 kcal/mol·M). Two mutants, W22L and W74F, have larger ΔG°_u values than the wild-type DHFR despite the smaller C_m values, due to the higher cooperativity of the transition (large negative m values). The other six mutants show smaller ΔG°_u values than the wild-type DHFR, with W133V showing an extremely small ΔG°_u value. These results clearly indicate that all tryptophan residues of DHFR play important roles in its structural stability.

Thermal Unfolding—Figure 5 shows far-ultraviolet CD

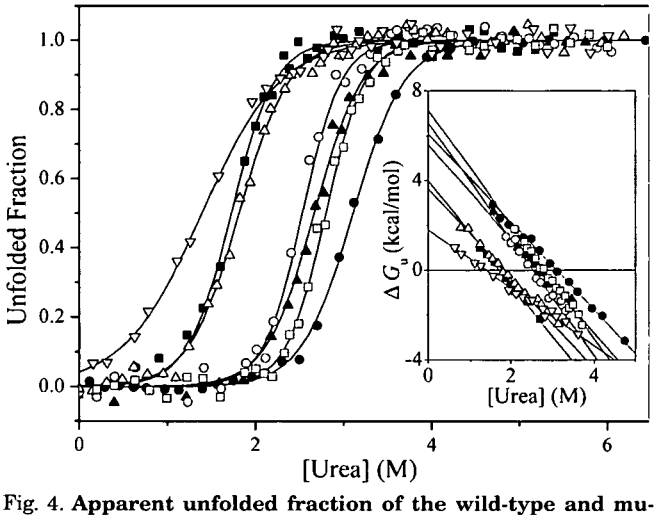

Fig. 4. **Apparent unfolded fraction of the wild-type and mutant DHFRs as a function of the urea concentration at 15°C.** The unfolded fraction was monitored by CD at 222 nm. The solvent used was 10 mM potassium phosphate (pH 7.0) containing 0.1 mM EDTA and 0.1 mM dithiothreitol. (●) Wild-type; (○) W22L; (△) W30L; (▲) W47L; (□) W74F; (■) W74L; (▽) W133V. Solid lines represent the theoretical fits to a two-state transition model with the parameter values shown in Table I. The inset in the figure show the dependence of the apparent free energy change of unfolding (ΔG_u) on the urea concentration.

TABLE I. **Thermodynamic parameters for urea unfolding of the wild-type and mutant DHFRs at 15°C.**[a]

DHFRs	ΔG°_u (kcal/mol)	m (kcal/mol·M)	C_m (M)
Wild-type[b]	6.08 ± 0.18	−1.96 ± 0.06	3.11
W22F	4.84 ± 0.11	−1.77 ± 0.04	2.73
W22L	6.58 ± 0.17	−2.60 ± 0.07	2.53
W30L	3.64 ± 0.14	−2.01 ± 0.07	1.81
W47L	5.60 ± 0.19	−2.10 ± 0.07	2.67
W74F	7.14 ± 0.28	2.55 ± 0.10	2.80
W74L	4.00 ± 0.18	−2.32 ± 0.09	1.72
W133F	5.25 ± 0.19	−2.14 ± 0.07	2.45
W133V	1.79 ± 0.25	−1.29 ± 0.09	1.39

[a]The solvent used was 10 mM potassium phosphate (pH 7.0) containing 0.1 mM EDTA and 0.1 mM dithiothreitol. The parameters ΔG°_u, m, and C_m were calculated with Eq. 2 by assuming a linear relationship between ΔG_u and the urea concentration. [b]Gekko *et al.* (*25*).

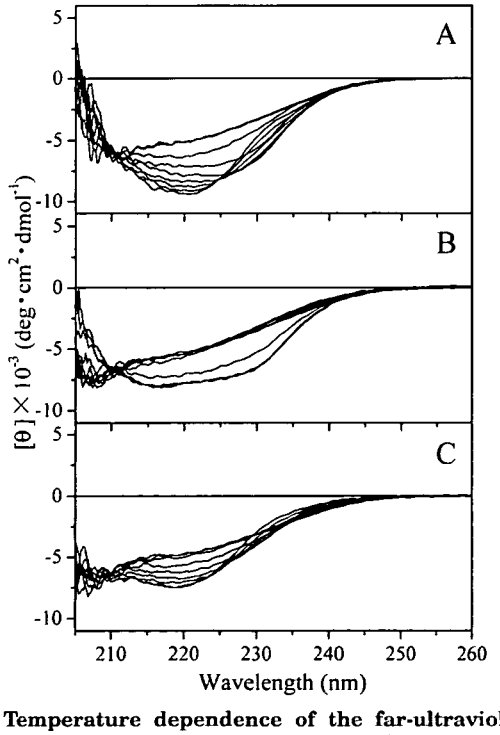

Fig. 5. **Temperature dependence of the far-ultraviolet CD spectra of W22F (A), W74L (B), and W133V (C) DHFRs.** The solvent used was 10 mM potassium phosphate (pH 7.0) containing 0.1 mM EDTA and 0.1 mM dithiothreitol. The spectra from bottom to top refer to the temperatures 5.5, 14.0, 23.8, 31.4, 39.6, 48.0, 56.1, 71.5, and 80.5°C in (A), to 5.3, 14.6, 25.4, 37.2, 46.6, 54.0, 63.3, 73.6, and 81.9°C in (B), and to 5.7, 14.7, 25.1, 34.9, 47.6, 56.3, 66.6, 74.0, and 82.6°C in (C).

Downloaded from http://jb.oxfordjournals.org/ at Islamic Azad University on September 30, 2012

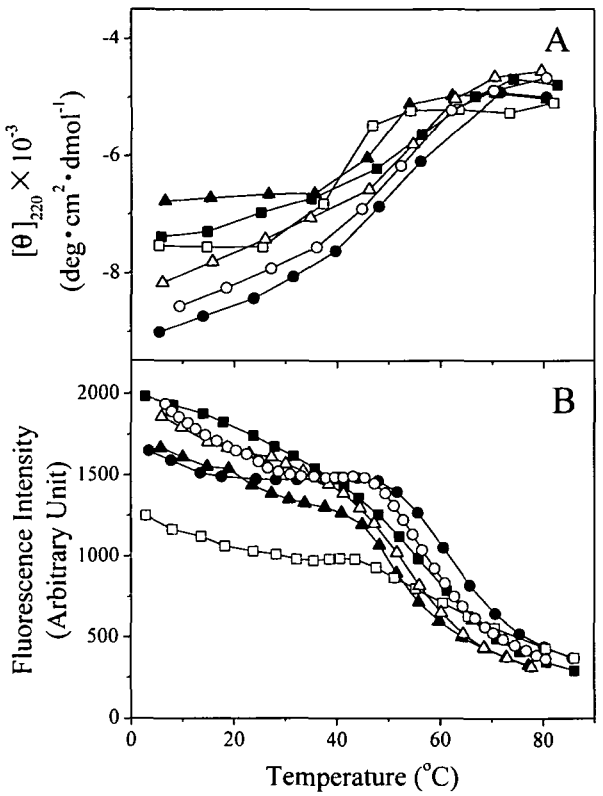

Fig. 6. **Temperature dependence of the CD intensity at 220 nm (A) and the fluorescence intensity at 345 nm (B) of the wild-type and mutant DHFRs.** The solvent used was 10 mM potassium phosphate (pH 7.0) containing 0.1 mM EDTA and 0.1 mM dithiothreitol. (○) Wild-type; (●) W22F; (△) W30L; (▲) W47L; (□) W74L; (■) W133V.

spectra of W22F, W74L, and W133V mutants at various temperatures. Thermal unfolding clearly occurs in the temperature range examined, as found for the wild-type DHFR (*30*). Reversibility of the thermal unfolding is estimated to be 85–90 % from the recovery of the CD intensity after cooling. Other mutants show similar temperature dependence and reversibility of the CD spectra. As typically observed for W22F mutant (Fig. 5A), there are two isoellipticity points at 225 and 210 nm in the CD spectra at 5–32°C. Similar spectra are also observed for W22L, W30L and W133F, although the first isoellipticity point (225 nm) shifts to 227 nm for W30L. In the case of W133V, another isoellipticity point appears at 235 nm besides 225 and 210 nm at 40–80°C (Fig. 5C). A common feature of these CD spectra is that an approximately equivalent increase and decrease in the CD intensity occur in the wavelength regions above and below 225 nm, respectively. On the other hand, the far-ultraviolet CD spectrum of W74L has only one isoellipticity point at 210 nm over the temperature range examined (Fig. 5B). Similar spectra are observed for W47L and W74F mutants. These results indicate that there exists an intermediate in the thermal unfolding process of these mutants as well as the wild-type DHFR (*30*), and that the Trp47-Trp74 exciton coupling is disrupted at 5–35°C before the main thermal unfolding occurs.

Figure 6 shows the temperature dependence of the molar ellipticity at 220 nm ($[\theta]_{220}$) and the fluorescence intensity at 345 nm for the wild-type and five mutant DHFRs.

TABLE II. **Specific and relative activities of the wild-type and mutant DHFRs at 25°C.**[a]

DHFRs	Specific activity (s^{-1})	Relative activity (%)[b]
Wild-type	14.3	100
W22F	7.2	50
W22L	1.9	13
W30L	9.1	64
W47L	15.5	108
W74F	12.6	88
W74L	9.4	66
W133F	12.6	88
W133V	7.4	52

[a]The solvent used was 33 mM succinic acid containing 44 mM imidazole, 44 mM diethanolamine, 60 μM NADPH, and 50 μM dihydrofolate (pH 7.0). The final concentrations of enzymes were 60–90 nM. The initial velocities of the enzyme reaction were calculated from the time course of absorbance at 340 nm using a differential molar extinction coefficient of 11,800 $M^{-1}\cdot cm^{-1}$ (*37*). [b]The specific activity of the wild-type DHFR was taken as 100%.

Although detailed thermodynamic analysis of thermal unfolding is outside the scope of this study, it is evident that the transition curve is significantly influenced by mutations, the transition temperature ranging over 10°C. In most cases, $[\theta]_{220}$ gradually increases with temperature in the range 5–35°C, followed by the large increase due to main unfolding transition in the range 40–70°C. In the same temperature range, the fluorescence intensity of all mutants except W133V shows the two-phase transition: the first transition accompanying a large red-shift of the spectra at 30–45°C, and the second one accompanying a small red-shift at higher temperature which corresponds to the major transition in $[\theta]_{220}$ (Fig. 6B). The first transition disappears for W133V, probably because this mutant is partly unfolded even at 15°C. The more stable mutant W133F clearly shows the first transition (data not shown). Thus, the thermal unfolding of these tryptophan mutants first disrupts the tertiary structure accompanying exposure of some tryptophan residues to the solvent, and this is followed by a global unfolding of the secondary structure, as identified for wild-type DHFR (*30*).

Specific Activity—Table II lists the specific activity of DHFRs and its relative value to that of the wild-type DHFR at 25°C and pH 7.0. All the mutants except W22L (13%) retain more than 50% of the enzyme activity of wild-type DHFR. So five tryptophan residues of DHFR have no fatal effect on the enzymatic function.

DISCUSSION

As shown in this study, mutations at the five tryptophan residues of DHFR bring about considerable changes in the native structure, stability, and enzyme activity. A matter of concern is how the individual tryptophan residues contribute to the overall structure and properties of this enzyme.

Contribution of Tryptophan Residues to Far-Ultraviolet CD Spectra—It is well known that the CD spectra in the far-ultraviolet region reflect the secondary structure of proteins. However, the tertiary structure, especially side chain of aromatic residues, has been found to influence the peptide CD of some proteins (*38, 39*). A typical case is the exciton coupling between Trp47 and Trp74 side chains of DHFR, as experimentally found with a W74L mutant (*15*). The theoretical calculation based on the X-ray crystal

Downloaded from http://jb.oxfordjournals.org/ at Islamic Azad University on September 30, 2012

structure also predicts the contribution of other tryptophan residues to the peptide CD of DHFR (*29*): the difference CD spectra between the wild-type and four mutant DHFRs (W22L, W30L, W47L, and W133L) are characterized by a large positive peak centered at 225 nm (W22L), a positive peak centered at 223 nm (W30L), a couplet with negative and positive peaks centered at 220 and 235 nm (W47L), and a negative peak centered at 232 nm (W133L). Comparison of these theoretical predictions with the experimentally observed difference CD spectra of these mutants will be a good indicator of the contribution of each tryptophan residue to the peptide CD.

As shown in Fig. 7, the difference CD spectrum for W22L shows a small couplet centered at 220 nm. The difference CD spectrum for W22F shows only a small positive peak at 223 nm (data not shown). These results are inconsistent with the theoretical prediction, suggesting that Trp22 has little influence on the peptide CD of DHFR. This is probable because Trp22 is located in a Met20 loop, which has three different conformations in crystal structures depending on the ligands (*6*). Two-dimensional NMR spectroscopy of Trp22 shows a cross-peak of two distinct environments (*40*), indicating two interchangeable orientations of Trp22 in solution. Recent high pressure NMR study has revealed that the equilibrium between the two orientations is easily influenced by pressure as well as temperature (*41*). It may therefore be difficult to predict precisely the contribution of Trp22 to the peptide CD without taking into consideration the population of such orientations. The difference CD spectrum for W30L shows small negative peaks centered at 220 and 235 nm, and a large positive peak at wavelengths below 210 nm. These results also disagree with the theoretical prediction. This may be partly due to unknown structural changes as suggested by the large CD depression at 200–210 nm (Fig. 2), the relatively low stability for urea unfolding (Table I), and the shift of isoellipticity point due to thermal unfolding (Fig. 5).

The difference CD spectra for W47L and W74L distinctly show a couplet with negative and positive peaks centered at 220 and 232 nm, respectively, consistent with the theoretical prediction. This result is also consistent with the observation of Kuwajima *et al.* (*15*) for a W74L mutant, proving that the side chains of Trp47 and Trp74 undergo exciton coupling, which affects the far-ultraviolet CD spectrum of DHFR. The difference CD spectrum for W133V mutant shows a large negative peak centered at 230 nm, as theoretically predicted for W133L. A similar spectrum is also observed for W133F (data not shown). These results indicate that the side chain of Trp133 contributes substantially to the far-ultraviolet CD spectrum of DHFR. An interesting finding is that the CD spectrum of W133F mutant has a clear shoulder at around 235 nm (Fig. 2C), as found in the CD spectrum of the wild-type DHFR bound to its cofactor, NADPH (*26*). This suggests that the NADPH binding induces a conformational change that reduces the contribution of Trp133 to the peptide CD of the wild-type DHFR.

Non-Additive Contribution of Tryptophan Residues to Fluorescence Spectra—As shown in Fig. 3, the single-tryptophan mutations other than W133V induce a decrease in fluorescence intensity, in some cases accompanied by a small peak shift. This suggests that the quantum yield of each tryptophan residue is largely different, while the polarity around the residue is similar. It is of interest to what extent each tryptophan residue contributes to the fluorescence intensity. Figure 8 shows the difference fluorescence spectra between the wild-type DHFR and five single-tryptophan mutants (W22L, W30L, W47L, W74L, and W133F), which were calculated from the fluorescence spectra in Fig. 3. The sum of these five difference spectra is only 60% of the intensity experimentally observed for wild-type DHFR. This means that each tryptophan residue has no additive contribution to the fluorescence spectra. Such a non-additivity is mainly ascribed to the abnormally small contribution of Trp22, Trp30, and Trp133. This demonstrates that the exciton coupling of Trp47-Trp74 cooperatively perturbs the electronic state of this protein structure through the long-range interaction.

Large Contribution of Tryptophan Residues to Structural Stability—As shown in Table I, the structural stability of DHFR is significantly modified by mutations at five tryptophan resides. The stability of most mutants decreases, as expected from the decreased hydrophobic stabilizing effect

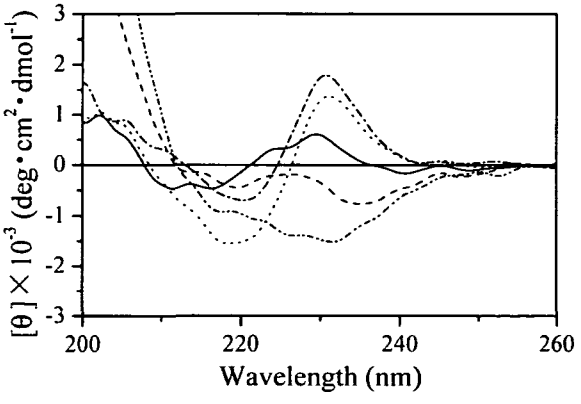

Fig. 7. **CD difference spectra between the wild-type and mutant DHFRs calculated from Fig. 2.** (——) Wild-type—W22L; (– – – –) wild-type—W30L; (------) wild-type—W47L; (–·–·–) wild-type—W74L; (–·–·–·–) wild-type—W133V.

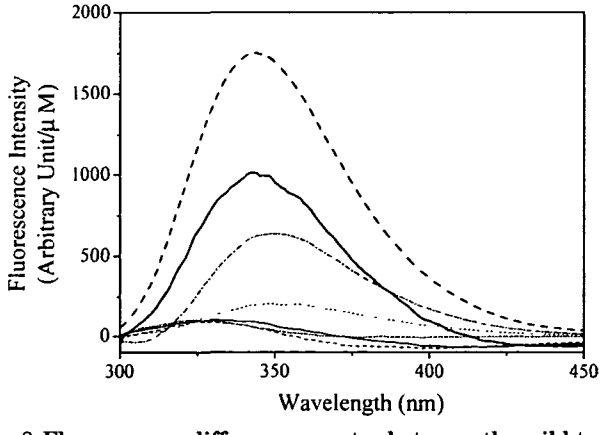

Fig. 8. **Fluorescence difference spectra between the wild-type and mutant DHFRs calculated from Fig. 3.** (——) Wild-type—W22L; (– – – –) wild-type—W30L; (------) wild-type—W47L; (–·–·–) wild-type—W74L; (–·–·–·–) wild-type—W133F. The sum of the above five difference spectra (——) is also indicated in comparison with the wild-type spectrum (– – –).

Downloaded from http://jb.oxfordjournals.org/ at Islamic Azad University on September 30, 2012

on the native structure. However, mutants W22L and W74F are more stable than the wild-type DHFR. W22L is more stable than W22F despite the low hydrophobicity of leucine relative to phenylalanine. There are two possible explanations for such a reverse hydrophobic effect on the stability. The first is that the nonpolar side chains are less exposed to the solvent in the unfolded state than in the native state, resulting in the stabilization of hydrophobic interaction of the unfolded state (*42*). This may be possible for mutations at a hyper or highly exposed position (*43*), but not in the present case, because the mutation sites (tryptophan residues) are buried in the interior of the protein molecule. As suggested by the CD and fluorescence spectra (Figs. 2 and 3), the native structure of DHFR is considerably modified by mutations, while the unfolded conformation seems to be essentially identical (Figs. 5 and 6). The effect of tryptophan mutations can thus be dominantly attributed to the native state. Replacement of tryptophan with any other amino acid should be accompanied by modification of not only the hydrophobic interaction but also the packness of the side chains. For W22L and W74F, the increased packness of the side chains would overcome the decreased hydrophobic interaction effect, leading to the increase in stability. Such a packing effect might partly contribute to destabilization of other mutants, typically W133V, in addition to the decreased hydrophobic effect. Detailed understanding of the stabilizing or destabilizing mechanism of these mutants must await the X-ray or NMR analyses of the native structure.

Structure of Intermediate in Thermal Unfolding—In a previous paper (*30*), we found that the acid and thermal unfolding of wild-type DHFR involves an equilibrium intermediate, and we predicted that the exciton coupling of Trp47-Trp74 might be disrupted and some tryptophan side chains exposed to the solvent in the intermediate state. This prediction was confirmed by the mutation of five tryptophan residues in the present work. Figures 5 and 6 clearly show that the thermal unfolding of tryptophan mutants as well as the wild-type DHFR consist of the two-phase transition involving an intermediate: the tertiary structure is disrupted accompanying the breaking of Trp47-Trp74 exciton coupling at 5–35°C, and this is followed by the main unfolding of peptide chains at 40–70°C. Characteristic mutation effects appear in the first transition in the low-temperature region rather than in the second one (Fig. 6). The first transition is not clearly observed for Trp47 and Trp74 mutants in the temperature dependence of $[\theta]_{220}$ (Fig. 6A), but this does not necessarily mean that the thermal unfolding of these mutants has no intermediate. The fluorescence-temperature plots clearly shows the first transition at 30–40°C for W47L and W74L (Fig. 6B), and more distinctly at 30–45°C for W74F (data not shown). Thus the intermediate state still exists in the thermal unfolding of mutants without Trp47-Trp74 exciton coupling. The small plateau in the fluorescence-temperature plots for W47L relative to W74L (Fig. 6B) suggests that the side chain of Trp47 is more exposed to the solvent than that of Trp74 in the intermediate state. W30L resembles W47L in having no distinct plateau in fluorescence-temperature plots, so the side chain of Trp30 may also be exposed to the solvent in the intermediate state.

Small Contribution of Tryptophan Residues to Enzyme Function—None of the mutations at the five tryptophan residues have a crucial effect on the enzymatic function of DHFR, although considerably large changes occur in the structure and stability. The most significant effect is seen for the mutation at Trp22, which is highly conserved in other bacterial and vertebrate DHFRs (*44*). This is probably because this position is very close (5 Å) to the active site Asp27 and located at the hinge of the Met20 loop, whose motion is essential for NADPH binding. It is noteworthy that the activity decreases in the order of wild-type > W22F > W22L, corresponding to the decreased hydrophobicity of the residue at position 22. Warren *et al.* also reported that the k_{cat} values of W22F and W22H are 87 and 6% of the wild-type value, respectively (*32*). These results suggest that the decreased activity of Trp22 mutants may be partly ascribed to the increased ionization or decreased pK_a of Asp27: the population of deionized carboxylic groups utilizable for the hydride transfer reaction would diminish, because the dielectric constant of the medium around Asp27 would increase as the hydrophobicity of the residues at position 22 decreases. However, such a decrease in activity with increasing residue hydrophobicity is also observed at positions 74 (wild-type > W74F > W74L) and 133 (wild-type > W133F > W133V). These positions are separated by 26 and 22 Å from Asp27, respectively, so it seems unlikely that their mutation directly influences the ionization of Asp27 through the medium effect. We need much more detailed information on the reaction kinetics of these mutants to understand the participation of long-range interaction or structural fluctuation in the enzymatic function.

To conclude, the five tryptophan residues in DHFR each make characteristic contributions to its structure, stability and function. Unusual spectroscopic behaviors of the native structure and the intermediate in thermal unfolding are mainly ascribed to the Trp47-Trp74 excimer, together with contributions of Trp30 and Trp133. None of the tryptophan residues has a critical role in the enzymatic function, but each plays an important role in the structural stability through the compensation effects of hydrophobic interaction and atomic packing. More detailed analyses on the native structure and enzyme kinetics of these tryptophan mutants would be fruitful for understanding the roles of the individual tryptophan residues.

We wish to thank the Nagoya University Computer Center for the use of the SALS program.

REFERENCES

1. Bystroff, C. and Kraut, J. (1991) Crystal structure of unliganded *Escherichia coli* dihydrofolate reductase. Ligand-induced conformational changes and cooperativity in binding. *Biochemistry* **30**, 2227–2239
2. Bolin, J.T., Filman, D.J., Matthews, D.A., Hamlin, R.C., and Kraut, J. (1982) Crystal structures of *Escherichia coli* and *Lactobacillus casei* dihydrofolate reductase refined at 1.7 Å resolution. I. General features and binding of methotrexate. *J. Biol. Chem.* **257**, 13650–13662
3. Bystroff, C., Oatley, S.J., and Kraut, J. (1990) Crystal structures of *Escherichia coli* dihydrofolate reductase: the $NADP^+$ holoenzyme and the folate-$NADP^+$ ternary complex. Substrate binding and a model for the transition state. *Biochemistry* **29**, 3263–3277
4. Reyes, V.M., Sawaya, M.R., Brown, K.A., and Kraut, J. (1995) Isomorphous crystal structures of *Escherichia coli* dihydrofolate reductase complexed with folate, 5-deazafolate, and 5,10-

Downloaded from http://jb.oxfordjournals.org/ at Islamic Azad University on September 30, 2012

dideazatetrahydrofolate: mechanistic implications. *Biochemistry* **34**, 2710–2723
5. Lee, H., Reyes, V.M., and Kraut, J. (1996) Crystal structures of *Escherichia coli* dihydrofolate reductase complexed with 5-formyltetrahydrofolate (folinic acid) in two space groups: evidence for enolization of pteridine O4. *Biochemistry* **35**, 7012–7020
6. Sawaya, M.R. and Kraut, J. (1997) Loop and subdomain movements in the mechanism of *Escherichia coli* dihydrofolate reductase: crystallographic evidence. *Biochemistry* **36**, 586–603
7. Falzone, C.J., Benkovic, S.J., and Wright, P.E. (1990) Partial ^{1}H NMR assignments of the *Escherichia coli* dihydrofolate reductase complex with folate: evidence for a unique conformation of bound folate. *Biochemistry* **29**, 9667–9677
8. Falzone, C.J., Wright, P.E., and Benkovic, S.J. (1991) Evidence for two interconverting protein isomers in the methotrexate complex of dihydrofolate reductase from *Escherichia coli*. *Biochemistry* **30**, 2184–2191
9. Epstein, D.M., Benkovic, S.J., and Wright, P.E. (1995) Dynamics of the dihydrofolate reductase-folate complex: catalytic sites and regions known to undergo conformational change exhibit diverse dynamical features. *Biochemistry* **34**, 11037–11048
10. Fierke, C.A., Johnson, K.A., and Benkovic, S.J. (1987) Construction and evaluation of the kinetic scheme associated with dihydrofolate reductase from *Escherichia coli*. *Biochemistry* **26**, 4085–4092
11. Stone, S.R. and Morrison, J.F. (1988) Dihydrofolate reductase from *Escherichia coli*: the kinetic mechanism with NADPH and reduced acetylpyridine adenine dinucleotide phosphate as substrates. *Biochemistry* **27**, 5493–5499
12. Morrison, J.F. and Stone, S.R. (1988) Mechanism of the reaction catalyzed by dihydrofolate reductase from *Escherichia coli*: pH and deuterium isotope effects with NADPH as the variable substrate. *Biochemistry* **27**, 5499–5506
13. Touchette, N.A., Perry, K.M., and Matthews, C.R. (1986) Folding of dihydrofolate reductase from *Escherichia coli*. *Biochemistry* **25**, 5445–5452
14. Frieden, C. (1990) Refolding of *Escherichia coli* dihydrofolate reductase: sequential formation of substrate binding sites. *Proc. Natl. Acad. Sci. USA* **87**, 4413–4416
15. Kuwajima, K., Garvey, E.P., Finn, B.E., Matthews, C.R., and Sugai, S. (1991) Transient intermediates in the folding of dihydrofolate reductase as detected by far-ultraviolet circular dichroism spectroscopy. *Biochemistry* **30**, 7693–7703
16. Jennings, P.A., Finn, B.E., Jones, B.E., and Matthews, C.R. (1993) A reexamination of the folding mechanism of dihydrofolate reductase from *Escherichia coli*: verification and refinement of a four-channel model. *Biochemistry* **32**, 3783–3789
17. Jones, B.E., Jennings, P.A., Pierre, R.A., and Matthews, C.R. (1994) Development of nonpolar surfaces in the folding of *Escherichia coli* dihydrofolate reductase detected by 1-anilinonaphthalene-8-sulfonate binding. *Biochemistry* **33**, 15250–15258
18. Jones, B.E., Beechem, J.M., and Matthews, C.R. (1995) Local and global dynamics during the folding of *Escherichia coli* dihydrofolate reductase by time-resolved fluorescence spectroscopy. *Biochemistry* **34**, 1867–1877
19. Hoeltzli, S.D. and Frieden, C. (1996) Real-time refolding studies of 6-^{19}F-tryptophan labeled *Escherichia coli* dihydrofolate reductase using stopped-flow NMR spectroscopy. *Biochemistry* **35**, 16843–16851
20. Clark, A.C. and Frieden, C. (1997) GroEL-mediated folding of structurally homologous dihydrofolate reductases. *J. Mol. Biol.* **268**, 512–525
21. Clark, A.C. and Frieden, C. (1999) Native *Escherichia coli* and murine dihydrofolate reductases contain late-folding non-native structures. *J. Mol. Biol.* **285**, 1765–1776
22. Birdsall, B., Feeney, S.J. B., Tendler, S.J., Hammond, D.J., and Roberts, G.C.K. (1989) Dihydrofolate reductase: multiple conformations and alternative modes of substrate binding. *Biochemistry* **28**, 2297–2305
23. Li, L., Falzone, C.J., Wright, P.E., and Benkovic, S.J. (1992) Functional role of a mobile loop of *Escherichia coli* dihydrofolate reductase in transition-state stabilization. *Biochemistry* **32**, 7826–7833
24. Gekko, K., Yamagami, K., Kunori, Y., Ichihara, S., Kodama, M., and Iwakura, M. (1993) Effects of point mutation in a flexible loop on the stability and enzymatic function of *Escherichia coli* dihydrofolate reductase. *J. Biochem.* **113**, 74–80
25. Gekko, K., Kunori, Y., Takeuchi, H., Ichihara, S., and Kodama, M. (1994) Point mutations at glycine-121 of *Escherichia coli* dihydrofolate reductase: important roles of a flexible loop in the stability and function. *J. Biochem.* **116**, 34–41
26. Ohmae, E., Iriyama, K., Ichihara, S., and Gekko, K. (1996) Effects of point mutations at the flexible loop glycine-67 of *Escherichia coli* dihydrofolate reductase on its stability and function. *J. Biochem.* **119**, 703–710
27. Ohmae, E., Ishimura, K., Iwakura, M., and Gekko, K. (1998) Effects of point mutations at the flexible loop alanine-145 of *Escherichia coli* dihydrofolate reductase on its stability and function. *J. Biochem.* **123**, 839–846
28. Ohmae, E., Iriyama, K., Ichihara, S., and Gekko, K. (1998) Nonadditive effects of double mutations at the flexible loops, glycine-67 and glycine-121, of *Escherichia coli* dihydrofolate reductase on its stability and function. *J. Biochem.* **123**, 33–41
29. Grishina, I.B. and Woody, R.W. (1994) Contributions of tryptophan side chains to the circular dichroism of globular proteins: exciton couplets and coupled oscillators. *Faraday Discuss.* **99**, 245–262
30. Ohmae, E., Kurumiya, T., Makino, S., and Gekko, K. (1996) Acid and thermal unfolding of *Escherichia coli* dihydrofolate reductase. *J. Biochem.* **120**, 946–953
31. Kamiyama, T., Ohmae, E., and Gekko, K. (1999) Large flexibility of dihydrofolate reductase as revealed by temperature effects on the volume and compressibility. *Chem. Lett.* **1999**, 507–508
32. Warren, M.S., Brown, K.A., Farnum, M.F., Howell, E.E., and Kraut, J. (1991) Investigation of the functional role of tryptophan-22 in *Escherichia coli* dihydrofolate reductase by site-directed mutagenesis. *Biochemistry* **30**, 11092–11103
33. Iwakura, M., Jones, B.E., Luo, J., and Matthews, C.R. (1995) A strategy for testing the suitability of cysteine replacements in dihydrofolate reductase from *Escherichia coli*. *J. Biochem.* **117**, 480–488
34. Vieira, J. and Messing, J. (1987) Production of single-stranded plasmid DNA in *Methods in Enzymology* (Wu, R. and Grossman, L., eds.) Vol. 153, pp. 3–11, Academic Press, New York
35. Nakagawa, T. and Oyanagi, Y. (1980) in *Recent Developments in Statistical Inference and Data Analysis* (Matsushita, K., ed.) pp. 221–225, North Holland Publishing Company, Amsterdam
36. Pace, C.N. (1986) Determination and analysis of urea and guanidine hydrochloride denaturation curves in *Methods in Enzymology* (Hirs, C.H.W. and Timasheff, S.N., eds.) Vol. 131, pp. 267–280, Academic Press, New York
37. Stone, S.R. and Morrison, J.F. (1982) Kinetic mechanism of the reaction catalyzed by dihydrofolate reductase from *Escherichia coli*. *Biochemistry* **21**, 3757–3765
38. Arnold, G.E., Day, L.A., and Dunker, A.K. (1992) Tryptophan contributions to the unusual circular dichroism of fd bacteriophage. *Biochemistry* **31**, 7948–7956
39. Vuilleumier, S., Sancho, J., Loewenthal, R., and Fersht, A.R. (1993) Circular dichroism studies of barnase and its mutants: characterization of the contribution of aromatic side chains. *Biochemistry* **32**, 10303–10313
40. Falzone, C.J., Wright, P.E., and Benkovic, S.J. (1994) Dynamics of a flexible loop in dihydrofolate reductase from *Escherichia coli* and its implication for catalysis. *Biochemistry* **33**, 439–442
41. Kitahara, R., Sareth, S., Yamada, H., Ohmae, E., Gekko, K., and Akasaka, K. (2000) High pressure NMR reveals active-site hinge motion of folate-bound *Escherichia coli* dihydrofolate reductase. *Biochemistry* **39**, 12789–12795
42. Pakula, A.A. and Sauer, R.T. (1990) Reverse hydrophobic effects relieved by amino-acid substitutions at a protein surface. *Nature* **344**, 363–364

Downloaded from http://jb.oxfordjournals.org/ at Islamic Azad University on September 30, 2012

43. Bowler, B.E., May, K., Zaragoza, T., York, P., Tong, A., and Caughey, W.S. (1993) Destabilizing effects of replacing a surface lysine of cytochrome c with aromatic amino acids: implications for the denatured state. *Biochemistry* **32**, 183–190
44. Volz, K.W., Matthews, D.A., Alden, R.A., Freer, S.T., Hansch, C., Kaufman, B.T., and Kraut, J. (1982) Crystal structure of avian dihydrofolate reductase containing phenyltriazine and NADPH. *J. Biol. Chem.* **257**, 2528–2536
45. Kraulis, P.J. (1991) MOLSCRIPT: a program to produce both detailed and schematic plots of protein structures. *J. Appl. Crystallogr.* **24**, 946–950

Downloaded from http://jb.oxfordjournals.org/ at Islamic Azad University on September 30, 2012